Article

Frequency combs induced by phase turbulence

https://doi.org/10.1038/s41586-020-2386-6

Received: 9 November 2019

Accepted: 18 March 2020

Published online: 17 June 2020

Check for updates

Marco Piccardo[1,2,8]✉, Benedikt Schwarz[1,3,8], Dmitry Kazakov[1], Maximilian Beiser[3], Nikola Opačak[3], Yongrui Wang[4], Shantanu Jha[1,5], Johannes Hillbrand[1,3], Michele Tamagnone[1], Wei Ting Chen[1], Alexander Y. Zhu[1], Lorenzo L. Columbo[6,7], Alexey Belyanin[4] & Federico Capasso[1]✉

Wave instability—the process that gives rise to turbulence in hydrodynamics[1]—represents the mechanism by which a small disturbance in a wave grows in amplitude owing to nonlinear interactions. In photonics, wave instabilities result in modulated light waveforms that can become periodic in the presence of coherent locking mechanisms. These periodic optical waveforms are known as optical frequency combs[2–4]. In ring microresonator combs[5,6], an injected monochromatic wave becomes destabilized by the interplay between the resonator dispersion and the Kerr nonlinearity of the constituent crystal. By contrast, in ring lasers instabilities are considered to occur only under extreme pumping conditions[7,8]. Here we show that, despite this notion, semiconductor ring lasers with ultrafast gain recovery[9,10] can enter frequency comb regimes at low pumping levels owing to phase turbulence[11]—an instability known to occur in hydrodynamics, superconductors and Bose–Einstein condensates. This instability arises from the phase–amplitude coupling of the laser field provided by linewidth enhancement[12], which produces the needed interplay of dispersive and nonlinear effects. We formulate the instability condition in the framework of the Ginzburg–Landau formalism[11]. The localized structures that we observe share several properties with dissipative Kerr solitons, providing a first step towards connecting semiconductor ring lasers and microresonator frequency combs[13].

Following decades of studies, the development of optical frequency combs continues at a rapid pace[4,6,14]. Research on frequency combs started from tabletop optical systems—such as Ti:sapphire mode-locked lasers, which revolutionized optical metrology[2]—the subsequent advances in the processing of semiconductor and dielectric materials led to much more compact frequency comb generators. Technological progress went hand in hand with many new applications, such as in spectroscopy and chemical sensing, arbitrary radiofrequency waveform generation, optical communications and quantum information. Within the realm of integrated optics, of particular interest are two classes of generators: semiconductor lasers and passive microresonators[6,15]; in the latter, the pump is an external continuous-wave laser and the gain stems from the Kerr nonlinearity. In both cases, the device starts from single-frequency operation, corresponding to the first lasing mode or the external pump. To generate a frequency comb, mechanisms capable of creating modes at different frequencies, coupling them and locking their phases need to be present in the cavity. In microresonators, above the parametric instability threshold, the external pump induces the appearance of sidebands, which grow and proliferate[16] through cascaded parametric processes. This coherent nonlinear process gives rise to phase-locked frequency combs. In Fabry–Pérot semiconductor lasers, multimode operation results from inhomogeneous gain saturation. A standing wave created by the first lasing mode (Fig. 1a) leads to a spatially varying distribution of the gain—a phenomenon known as spatial hole burning (SHB). In a dispersive cavity, SHB leads to the proliferation of modes with nonequidistant frequencies, where phase locking can be achieved through the nonlinearity of the gain medium itself[17–20].

SHB is not expected to form in a ring cavity, as the clockwise and counterclockwise modes of a ring resonator are not naturally coupled in the absence of a well defined reflection point that breaks the circular symmetry. We show that semiconductor ring lasers[21–23] can nevertheless undergo a single-mode instability owing to a phenomenon known in the realm of the Ginzburg–Landau theory as phase turbulence[11] and form frequency combs even in the absence of spatial or spectral hole burning. Multimode emission and comb formation occur at a pumping level fractionally higher than the lasing threshold. This is in contrast to the Risken–Nummedal–Graham–Haken instability, which also promotes multimode operation of a ring laser but at a non-practical pumping level of at least nine times above the threshold[7,8].

Ring frequency combs

To study phase turbulence in lasers, we use ring quantum cascade lasers (QCLs)[9]. These are monolithic frequency comb generators that

[1]Harvard John A. Paulson School of Engineering and Applied Sciences, Harvard University, Cambridge, MA, USA. [2]Center for Nano Science and Technology, Fondazione Istituto Italiano di Tecnologia, Milan, Italy. [3]Institute of Solid State Electronics, TU Wien, Vienna, Austria. [4]Department of Physics and Astronomy, Texas A&M University, College Station, TX, USA. [5]Physics Department, Yale University, New Haven, CT, USA. [6]Dipartimento di Elettronica e Telecomunicazioni, Politecnico di Torino, Turin, Italy. [7]Consiglio Nazionale delle Ricerche, CNR-IFN, Bari, Italy. [8]These authors contributed equally: Marco Piccardo, Benedikt Schwarz.. ✉e-mail: piccardo@g.harvard.edu; capasso@seas.harvard.edu

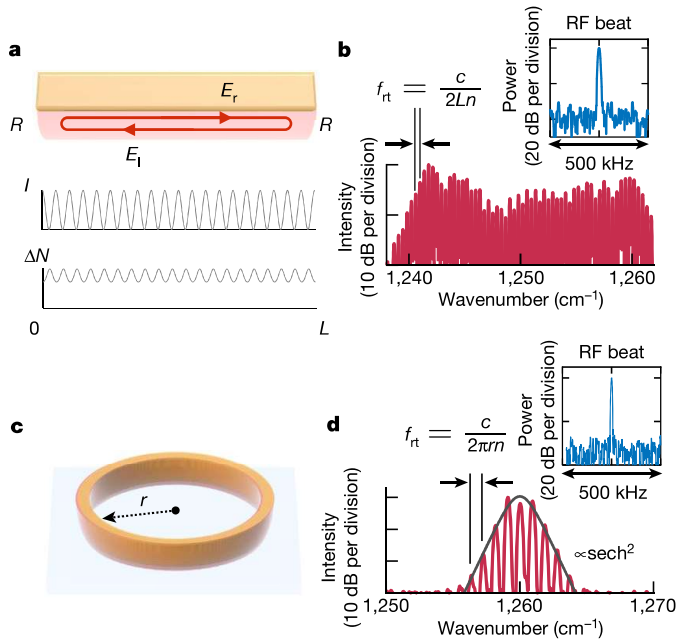

Fig. 1 | Fabry–Pérot and ring frequency combs. a, Schematic of a Fabry–Pérot cavity with rightward (E_r) and leftward (E_l) propagating waves coupled through facets of reflectivity R. As a result of the counterpropagating waves, optical standing waves of intensity I and a static grating of population inversion ΔN are formed in the cavity of length L. **b**, Experimental optical spectrum of a Fabry–Pérot frequency comb generated from a QCL (L = 3.7 mm). The round-trip frequency (f_{rt}) defines the comb spacing (11.5 GHz), which is shown in the inset. **c**, Schematic of a monolithic semiconductor ring laser of radius r. **d**, Experimental optical spectrum of a ring QCL frequency comb (r = 500 μm). The envelope of the spectrum is fitted to a sech^2 function for the discussion on solitonic structures. Also shown is the narrow electrical beat note of the laser (central frequency 27.8 GHz). The two lasers are fabricated from the same material. The resolution of the optical spectrum analyser is 3 GHz in **b** and 6 GHz in **d**, and the resolution bandwidth of the radiofrequency (RF) spectrum analyser is 9.1 kHz in **b** and 5.6 kHz in **d**.

combine nonlinearity and gain[10] and have applications in dual-comb spectroscopy[24], metrology[25] and microwave photonics[26]. QCL frequency combs typically have the Fabry–Pérot geometry (Fig. 1a) and serve the mid-infrared and terahertz regions of the electromagnetic spectrum, which are strategic for chemical sensing. They have the advantages of broad tunability, through band-structure engineering, and high portability because they are electrically pumped and compact. Here we fabricate ring QCLs in a ridge waveguide geometry (Fig. 1c). These ring QLCs emit in the mid-infrared and operate at room temperature under constant electrical injection (Methods). A small fraction of light can escape from the ring cavity owing to scattering, allowing us to perform a spectral characterization.

We find that at an injection level only fractionally higher than the lasing threshold J_{th} (typically $1.1J_{th}$–$1.5J_{th}$), the ring lasers undergo a transition to a multimode regime (Fig. 1d) that is distinctly different from those observed in Fabry–Pérot QCLs (Fig. 1b). The optical spectrum of the ring has fewer modes and exhibits a bell-shaped envelope. As in Fabry–Pérot resonators, the modes are separated by the round-trip frequency of the cavity $f_{rt} = c/(2\pi rn)$, where r is the ring radius, n = 3.4 is the effective refractive index of the waveguide and c is the speed of light in vacuum. The coherence of the state is manifested by its narrow beat note (Supplementary Fig. 2), which indicates its frequency comb nature, further confirmed by a coherent beat note detection technique (Extended Data Fig. 1). A notable feature of the instability is that as the current in the device is increased, the laser can revert back to single-mode operation (Extended Data Fig. 2)—a feature not observed in regular Fabry–Pérot lasers. A multimode instability close to the threshold has been reported also for a ring dye laser[27] but with different features, namely, suppression of the resonant mode and a parametric gain of two side modes separated by about the Rabi frequency.

Ginzburg–Landau theory

To support the experimental evidence of multimode operation, we reexamine the theory of lasers with fast gain media. We show that ring frequency combs can be explained on the basis of a phase instability that affects the single-mode solution of the complex Ginzburg–Landau equation (CGLE)[11,28]. The CGLE is a nonlinear differential equation that describes spatially extended systems of coupled nonlinear oscillators. It appears in many branches of physics, such as superconductivity, Bose–Einstein condensation and quantum field theory. In semiconductor laser theory, it can be shown that the field dynamics is described by a CGLE assuming fast gain relaxation[29]. Although fast relaxation is not applicable to a conventional bipolar semiconductor laser (diode laser), it is a well known property of QCLs. From the master equation of lasers with fast gain media[20] we derive the CGLE for the laser field E:

$$\partial_t E = E + (1 + ic_D)\partial_z^2 E - (1 + ic_{NL})|E|^2 E \quad (1)$$

where t is the time and z is the spatial coordinate running along the ring cavity (see Supplementary Information for the analytical derivation). The only two parameters of the equation are c_D and c_{NL}, which control the stability of the system and relate to dispersive and nonlinear effects, respectively. In the case of QCLs, c_D depends on the group velocity dispersion (GVD), and c_{NL} depends on the Kerr coefficient. Although the bulk Kerr nonlinearity of a semiconductor crystal is small, its contribution is compensated by a term of the same order given by the linewidth enhancement factor (LEF)[12,20]. Despite its different nature from the Kerr nonlinearity, the LEF enters both the c_D and c_{NL} terms and provides the phase-amplitude coupling needed for the phase instability.

In CGLE theory, the parameter space spun by c_D and c_{NL} is divided into different stability regions by the Benjamin–Feir lines[11,30], which are defined by $1 + c_D c_{NL} = 0$. The inner region confined by the lines has stable, purely single-mode solutions, whereas the solutions lying in the two outer regions exhibit a phase instability[29], which makes them multimode. We investigate the spectral content of the laser field solutions according to their location in the CGLE parameter space. In Fig. 2a we show the result of space–time domain simulations of a ring QCL for different points in the (c_D, c_{NL}) parameter space determined by typical laser parameters (Extended Data Table 1). In these numerical simulations we use the full laser model without approximations[20], and the CGLE is used only to guide the choice of laser parameters, allowing us to probe solutions in various points of the parameter space. The computed optical spectra confirm that in the stable region (white) only single-mode solutions are supported, whereas in the instability regions (red) the laser attains a multimode regime despite the absence of SHB, as already suggested by a recent theory of ring QCLs based on the effective Maxwell–Bloch equations[31]. The (c_D, c_{NL}) coordinates corresponding to our laser parameters, as obtained from the GVD and LEF measurements (Fig. 2c, d), are marked in Fig. 2a and show that the experimentally observed multimode instability is compatible with the phase turbulence mechanism.

Emergence of order from turbulence

Space–time simulations allow us to resolve the full temporal evolution of the laser (Fig. 2b, Supplementary Video). Starting from spontaneous emission, discontinuous changes of the laser field are produced. Amplitude fluctuations of the first lasing mode are coupled to phase fluctuations via the LEF or α parameter $\alpha = (\partial n'/\partial N)/(\partial n''/\partial N)$, where n' and n'' are the real and imaginary parts of the refractive index, respectively, and N is the carrier density[12]. Physically, fluctuations of n' in the QCL active region lead to fluctuations in the spacing between the lasing

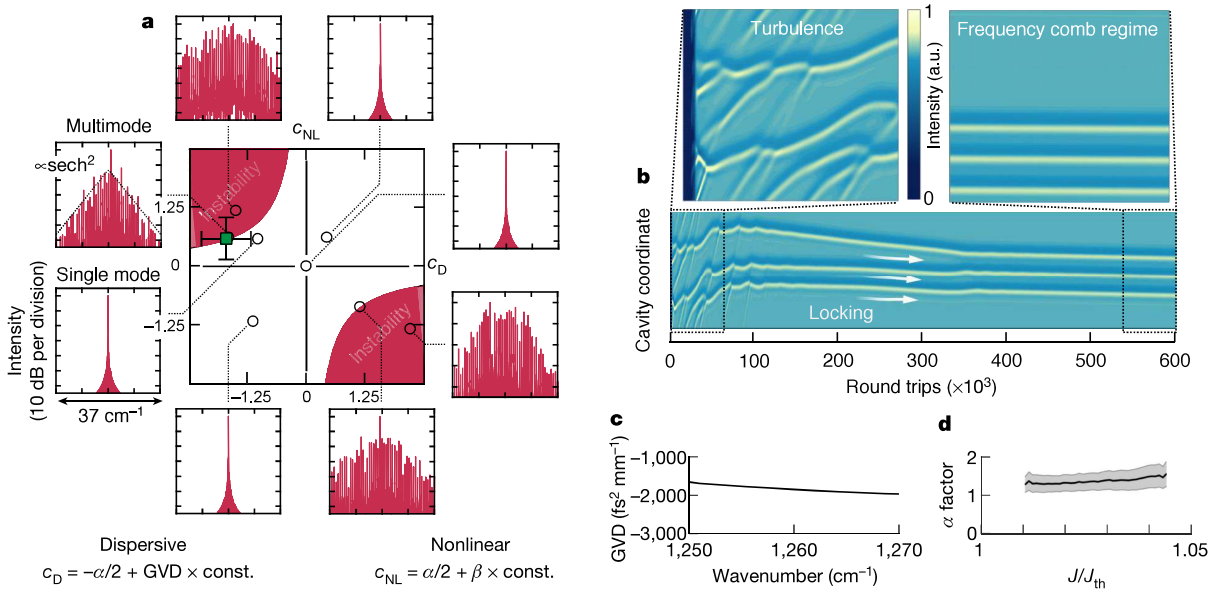

Fig. 2 | Conditions for the phase instability in a monolithic ring laser. **a**, Theoretical spectra obtained by solving the laser master equation are shown for different points in parameter space, confirming the behaviour expected from Ginzburg–Landau theory. In the simulations, SHB is turned off, so the obtained multimode regimes are due to the Ginzburg–Landau phase instability. In all plots the *x* axis spans 50 longitudinal modes of the ring and the *y* axis shows intensity (10 dB per division). Also shown is the region corresponding to the experimental devices, as obtained from the laser parameters, with the related uncertainties corresponding to the standard deviation (square marker; Supplementary Table 1). In the simulated spectrum corresponding to this point, a sech^2 envelope was fitted to the envelope for the purposes of the discussion on solitonic structures (dashed line). The formulas shown in the inset are an approximation in the limit of small linewidth-enhancement factors (Supplementary Information). GVD is the group velocity dispersion, α is the linewidth enhancement factor and β is the Kerr nonlinearity, which is small in QCLs. **b**, Space–time simulation of the laser dynamics, showing the intensity in the ring cavity at every round trip. Starting from spontaneous emission (dark stripe in the left inset), the laser destabilizes into a turbulent regime and eventually reaches a frequency comb regime. The simulation solves the laser master equation for 600 million time steps (0.05 ms interval). The corresponding point in parameter space is indicated by the square marker in **a**. **c**, **d**, Measurement of two physical quantities entering c_D and c_{NL} for a ring QCL. In **d**, the experimental values are shown as a function of current density normalized to the lasing threshold. Error bars are obtained as the standard deviation of multiple (20) repeated measurements. a.u., arbitrary units.

mode and the side modes. The shifts of the latter with respect to the gain peak eventually lead to multimode lasing, despite the absence of SHB. In CGLE theory, the resulting dynamical behaviour shown in Fig. 2b is described as 'phase turbulence'. This regime is characterized by the presence of chaotic intensity fluctuations with small amplitude that never reach zero and by the absence of phase dislocations[32] (for a detailed discussion of the role of turbulence, see Supplementary Information). After a relatively long time interval (about 400,000 round trips) the laser reaches a frequency comb regime, where the intensity becomes periodic, with the waveform repeating itself at every round trip. Whereas phase turbulence provides a coupling mechanism among the modes via the LEF, which is alternative to SHB in Fabry–Pérot lasers, it is the semiconductor saturation nonlinearity via four-wave mixing that, for a sufficiently high intracavity field, becomes efficient at compensating dispersion through a self-injection mechanism[10]. Besides the conventional description in terms of LEF and GVD[20], the formation of the frequency comb can be described from the point of view of Ginzburg–Landau theory as the morphogenesis of a regular spatiotemporal pattern. Here the locking process manifests itself as the interaction of confined intensity structures that shift with respect to each other, eventually conforming into a single stable structure (Fig. 2b).

Role of intracavity defects

In demonstrating that phase turbulence lies at the heart of the multimode instability of ring lasers, it is essential to distinguish it from another mechanism that normally drives the instability, SHB. Here we show that in a ring cavity that supports SHB, the multimode instability leads to a completely different comb state. SHB arises in a cavity in the presence of a well defined reflection point that couples counterpropagating waves. Whereas in a Fabry–Pérot cavity the waves are naturally coupled owing to reflections off the cleaved facets, in a ring cavity an analogous reflection point—a defect—must be intentionally introduced. This is because unintentional defects, which may result from imperfections in fabrication, are insufficient to trigger the SHB instability (Supplementary Fig. 5). We embed a defect in a ring laser waveguide by means of focused ion beam lithography (Fig. 3a). A simple, yet effective, way of controlling the defect reflectivity is to etch a narrow slit across the waveguide to create an air gap in the active region of the laser (Fig. 3b). We choose a slit width of 0.5 µm that gives a reflectivity of $R \approx 22\%$, which is close to the facet reflectivity of an uncoated Fabry–Pérot QCL ($R = 29\%$). The defect-engineered laser generates a frequency comb with a spectrum that is drastically different from that of a ring without an intentional defect (Fig. 3c, Supplementary Fig. 6). The spectrum has an irregular envelope—the result of complex laser mode competition—similar to that of Fabry–Pérot devices, in which multimode operation is also dominated by SHB. The presence of optical standing waves enabling SHB is demonstrated by the beat note pattern measured along the cavity, with a maximum located, as expected, at the engineered defect (Fig. 3d, Extended Data Fig. 3, Supplementary Fig. 3). Space–time simulations of this laser confirm a different dynamics from that of non-defect-engineered rings. The instability shows large intensity fluctuations and a fragmented temporal evolution (Fig. 3e). Locking occurs over a shorter time interval (about 10,000 round trips) and results in a nearly flat intensity waveform, as in Fabry–Pérot QCL combs[20]. These results show that high reflectivity values, comparable to those of uncoated Fabry–Pérot resonators, are needed to mask the effects of phase turbulence in a ring and enable multimode emission due to SHB.

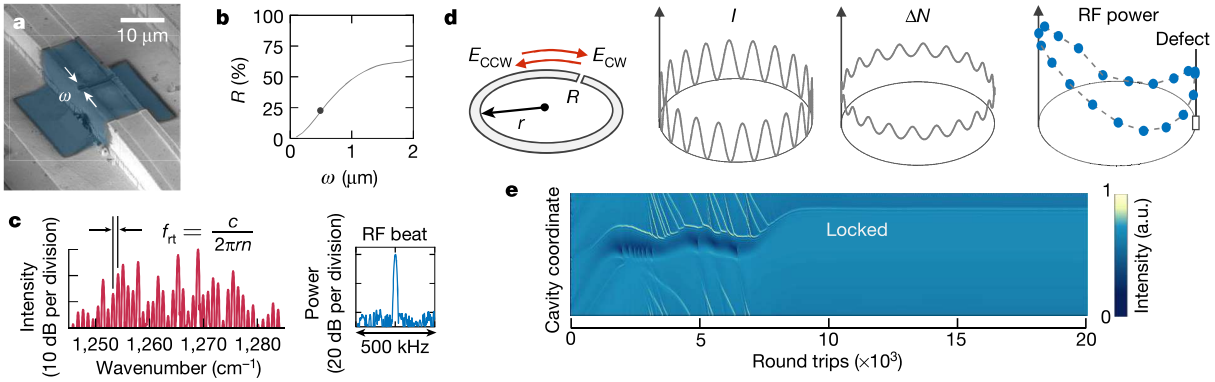

Fig. 3 | Defect-engineered ring frequency comb. a, Scanning electron microscope image of the defect-engineered ring laser, showing the aperture in the metal (blue region in false colour) with a slit width of $\omega = 0.5$ μm fabricated by focused ion beam lithography. **b**, Reflectivity induced by the slit as a function of its width, as calculated from numerical wave simulations (solid line). The reflectivity of the studied device is $R \approx 22\%$ (dot). **c**, Experimental optical spectrum of a defect-engineered ring QCL ($r = 500$ μm) fabricated from the same material as the other devices studied in this work. Also shown is the microwave beat note extracted from the laser (central frequency 27.8 GHz, resolution bandwidth 9.1 kHz). **d**, Schematic of a ring laser with an embedded engineered defect of reflectivity R. The defect induces clockwise (E_{CW}) and counterclockwise (E_{CCW}) waves, resulting in an optical standing wave of intensity I and a static population grating of population inversion ΔN. The right panel shows the experimental beat note power pattern (RF power) measured along the perimeter of the ring at the round-trip frequency indicating a bidirectional regime. **e**, Space–time simulation of a ring laser with a defect ($R = 25\%$).

Discussion

Linking the physics of ring lasers to the CGLE suggests a connection with Kerr-driven frequency comb generators. The latter are usually described by the Lugiato–Lefever equation[13] (LLE) with well known soliton solutions[33–36] derived from the CGLE with coherent forcing in the limit of large c_D and c_{NL} parameters. Moreover, we showed that the LEF, which enters both Ginzburg–Landau parameters in the case of a ring laser, adds up to the contributions of the Kerr nonlinearity and the GVD. The interplay of dispersive and nonlinear effects is essential to produce a self-starting instability, as in the case of the modulation instability that lies at the origin of Kerr solitons in microresonators[36].

The link with Kerr combs can be seen not only in the governing equations but also from the optical spectra. The bell-shaped envelope of the QCL ring comb spectra fits well to a sech^2 function (Figs. 1d, 2a), which is characteristic of dissipative Kerr solitons. The observation of spectral gaps in certain devices (Extended Data Figs. 2, 4) is also reminiscent of the variety of Kerr soliton spectra measured for different pump detuning conditions[33,34]. These observations indicate that the necessary conditions for the formation of solitonic structures[31] exist in ring QCLs, although proving their occurrence is a considerable experimental and theoretical undertaking that requires further investigation. It is known from Ginzburg–Landau theory that the CGLE can have localized structures, such as 'modulation amplitude waves'[37], as solutions, similarly to the LLE. These appear in the phase turbulence regime and exhibit weak amplitude modulations on a homogeneous background—features also observed in our numerical simulations of ring QCLs (Fig. 2b, Supplementary Fig. 1) and supported by the experimental characterization of the spectral phases of these lasers (Supplementary Information). In the simulations we find that the number of structures in states such as that shown in Fig. 2b vary stochastically with the initial conditions of the laser; by changing only the seed of the spontaneous emission noise and repeating the same simulation, we obtained a laser state with four structures instead of three (Extended Data Fig. 1). This is a clear indication of a multistability phenomenon, which is typical of dissipative solitons in extended systems such as Kerr microcombs.

We also highlight a historical analogy with the progress in the field of passive microresonators: prior theoretical studies by Lugiato and co-workers on transverse patterns in lasers[38,39], temporally contiguous with the well known work with Lefever on transverse patterns in passive optical systems[13], derived an equation with a mathematical form very similar to our CGLE, which however describes longitudinal patterns in ring lasers. This is reminiscent of the history of microresonators, in which the LLE anticipated the first experimental demonstration of Kerr combs[40], which also have longitudinal patterns and were later traced back to the LLE.

Besides the several analogies between the two classes of localized structures/combs in Kerr microresonators and ring QCLs highlighted so far, we believe that there exist a few fundamental differences that could imply different solitonic properties (for example, response to external addressing, mutual interaction), but the exhaustive study of which would require a dedicated future work. These mainly originate from the different kinds of nonlinearity providing the phase locking between competing modes and the absence of a forcing field in ring QCLs, which might give an advantage to these devices in terms of compactness. In fact, whereas the pumping of passive microresonators requires energy incoming through optical injection, which is responsible for the appearance of a strong central mode in the comb spectrum that is undesirable in many applications, QCL combs operate without an injected field. In this regard, QCLs are more similar to the recently demonstrated laser cavity–soliton microcombs[41]—Kerr microcavities nested in an amplifying fibre loop providing gain—but are more compact. A ring QCL acting as an electrically pumped microresonator would hold a substantial technological potential, in particular considering the strategic spectral ranges covered by QCLs. Further improvements in this direction should concentrate on the design of efficient light outcouplers—with the precaution of not perturbing the physics of the phase turbulence instability—and on the extension of the comb bandwidth that, unlike the case of Fabry–Pérot QCLs, is not limited by SHB, but only by the LEF and GVD.

Online content

Any methods, additional references, Nature Research reporting summaries, source data, extended data, supplementary information, acknowledgements, peer review information; details of author contributions and competing interests; and statements of data and code availability are available at https://doi.org/10.1038/s41586-020-2386-6.

1. Reynolds, O. XXIX. An experimental investigation of the circumstances which determine whether the motion of water shall be direct or sinuous, and of the law of resistance in parallel channels. *Philos. Trans. R. Soc. Lond.* **174**, 935–982 (1883).
2. Hänsch, T. W. Nobel lecture: passion for precision. *Rev. Mod. Phys.* **78**, 1297–1309 (2006).
3. Udem, T., Holzwarth, R. & Hänsch, T. W. Optical frequency metrology. *Nature* **416**, 233–237 (2002).
4. Picqué, N. & Hänsch, T. W. Frequency comb spectroscopy. *Nat. Photon.* **13**, 146–157 (2019).
5. Vahala, K. J. Optical microcavities. *Nature* **424**, 839–846 (2003).
6. Gaeta, A. L., Lipson, M. & Kippenberg, T. J. Photonic-chip-based frequency combs. *Nat. Photon.* **13**, 158–169 (2019).
7. Risken, H. & Nummedal, K. Self-pulsing in lasers. *J. Appl. Phys.* **39**, 4662–4672 (1968).
8. Graham, R. & Haken, H. Quantum theory of light propagation in a fluctuating laser-active medium. *Z. Phys.* **213**, 420–450 (1968).
9. Mujagić, E. et al. Grating-coupled surface emitting quantum cascade ring lasers. *Appl. Phys. Lett.* **93**, 011108 (2008).
10. Hugi, A., Villares, G., Blaser, S., Liu, H. C. & Faist, J. Mid-infrared frequency comb based on a quantum cascade laser. *Nature* **492**, 229–233 (2012).
11. Aranson, I. S. & Kramer, L. The world of the complex Ginzburg–Landau equation. *Rev. Mod. Phys.* **74**, 99–143 (2002).
12. Henry, C. Theory of the linewidth of semiconductor lasers. *IEEE J. Quantum Electron.* **18**, 259–264 (1982).
13. Lugiato, L. A. & Lefever, R. Spatial dissipative structures in passive optical systems. *Phys. Rev. Lett.* **58**, 2209–2211 (1987).
14. Kues, M. et al. Quantum optical microcombs. *Nat. Photon.* **13**, 170–179 (2019).
15. Kippenberg, T. J., Holzwarth, R. & Diddams, S. A. Microresonator-based optical frequency combs. *Science* **332**, 555–559 (2011).
16. Herr, T. et al. Universal formation dynamics and noise of Kerr-frequency combs in microresonators. *Nat. Photon.* **6**, 480–487 (2012).
17. Agrawal, G. P. Population pulsations and nondegenerate four-wave mixing in semiconductor lasers and amplifiers. *J. Opt. Soc. Am. B* **5**, 147–159 (1988).
18. Faist, J. et al. Quantum cascade laser frequency combs. *Nanophotonics* **5**, 272–291 (2016).
19. Piccardo, M. et al. The harmonic state of quantum cascade lasers: origin, control, and prospective applications. *Opt. Express* **26**, 9464–9483 (2018).
20. Opačak, N. & Schwarz, B. Theory of frequency-modulated combs in lasers with spatial hole burning, dispersion, and Kerr nonlinearity. *Phys. Rev. Lett.* **123**, 243902 (2019).
21. Matsumoto, N. & Kumabe, K. AlGaAs-GaAs semiconductor ring laser. *Jpn. J. Appl. Phys.* **16**, 1395–1398 (1977).
22. Krauss, T., Laybourn, P. J. R. & Roberts, J. CW operation of semiconductor ring lasers. *Electron. Lett.* **26**, 2095–2097 (1990).
23. Gelens, L. et al. Exploring multistability in semiconductor ring lasers: theory and experiment. *Phys. Rev. Lett.* **102**, 193904 (2009).
24. Villares, G., Hugi, A., Blaser, S. & Faist, J. Dual-comb spectroscopy based on quantum-cascade-laser frequency combs. *Nat. Commun.* **5**, 5192 (2014).
25. Consolino, L. et al. Fully phase-stabilized quantum cascade laser frequency comb. *Nat. Commun.* **10**, 2938 (2019).
26. Piccardo, M. et al. Radio frequency transmitter based on a laser frequency comb. *Proc. Natl Acad. Sci. USA* **116**, 9181–9185 (2019); correction **116** 17598 (2019).
27. Hillman, L. W., Krasiński, J., Boyd, R. W. & Stroud, C. R. Observation of higher order dynamical states of a homogeneously broadened laser. *Phys. Rev. Lett.* **52**, 1605–1608 (1984).
28. Staliunas, K. Laser Ginzburg–Landau equation and laser hydrodynamics. *Phys. Rev. A* **48**, 1573–1581 (1993).
29. Gil, L. & Lippi, G. L. Phase instability in semiconductor lasers. *Phys. Rev. Lett.* **113**, 213902 (2014).
30. Chate, H. Spatiotemporal intermittency regimes of the one-dimensional complex Ginzburg–Landau equation. *Nonlinearity* **7**, 185–204 (1994).
31. Columbo, L. L., Barbieri, S., Sirtori, C. & Brambilla, M. Dynamics of a broad-band quantum cascade laser: from chaos to coherent dynamics and mode-locking. *Opt. Express* **26**, 2829–2847 (2018).
32. Shraiman, B. et al. Spatiotemporal chaos in the one-dimensional complex Ginzburg–Landau equation. *Physica D* **57**, 241–248 (1992).
33. Kippenberg, T. J., Gaeta, A. L., Lipson, M. & Gorodetsky, M. L. Dissipative Kerr solitons in optical microresonators. *Science* **361**, eaan8083 (2018).
34. Herr, T. et al. Temporal solitons in optical microresonators. *Nat. Photon.* **8**, 145–152 (2014).
35. Cole, D. C., Lamb, E. S., Del'Haye, P., Diddams, S. A. & Papp, S. B. Soliton crystals in Kerr resonators. *Nat. Photon.* **11**, 671–676 (2017).
36. Karpov, M. et al. Dynamics of soliton crystals in optical microresonators. *Nat. Phys.* **15**, 1071–1077 (2019).
37. Brusch, L., Zimmermann, M. G., van Hecke, M., Bär, M. & Torcini, A. Modulated amplitude waves and the transition from phase to defect chaos. *Phys. Rev. Lett.* **85**, 86–89 (2000).
38. Lugiato, L. A., Oldano, C. & Narducci, L. M. Cooperative frequency locking and stationary spatial structures in lasers. *J. Opt. Soc. Am. B* **5**, 879–888 (1988).
39. Kaige, W., Abraham, N. B. & Lugiato, L. A. Leading role of optical phase instabilities in the formation of certain laser transverse patterns. *Phys. Rev. A* **47**, 1263–1273 (1993).
40. Del'Haye, P. et al. Optical frequency comb generation from a monolithic microresonator. *Nature* **450**, 1214–1217 (2007).
41. Bao, H. et al. Laser cavity-soliton microcombs. *Nat. Photon.* **13**, 384–389 (2019).